

## Electronic structure close to the Fermi energy of $KC_{60}$ at room temperature

This article has been downloaded from IOPscience. Please scroll down to see the full text article.

1997 J. Phys.: Condens. Matter 9 11151

(<http://iopscience.iop.org/0953-8984/9/50/016>)

View [the table of contents for this issue](#), or go to the [journal homepage](#) for more

Download details:

IP Address: 171.66.16.209

The article was downloaded on 14/05/2010 at 11:50

Please note that [terms and conditions apply](#).

## Electronic structure close to the Fermi energy of $\text{KC}_{60}$ at room temperature

A Gutiérrez† and S L Molodtsov‡

† Departamento de Corrosión y Protección, Centro Nacional de Investigaciones Metalúrgicas (CENIM), CSIC, Avenida Gregorio del Amo 8, E-28040 Madrid, Spain

‡ Institut für Oberflächen und Mikrostrukturphysik, Technische Universität Dresden, Mommsenstrasse 13, D-01062 Dresden, Germany

Received 30 May 1997, in final form 16 September 1997

**Abstract.** We report on a photoemission (PE) study of the region close to the Fermi energy ( $E_F$ ) in  $\text{K}_x\text{C}_{60}$  ( $0 < x \leq 3$ ). The partially filled LUMO-derived band consists of two peaks separated in energy by  $\sim 1$  eV. Variations in the PE cross sections cause these peaks to be resolved only for certain photon energies. The peak at higher binding energy predominates at very low  $x$  but its intensity gradually decreases when  $x$  increases, until for  $x \geq 2$  it has almost disappeared. This component is assigned to a room temperature dimeric or polymeric  $\text{KC}_{60}$  phase. The peak at lower binding energy is very similar to the LUMO-derived band of  $\text{K}_3\text{C}_{60}$ , but with a slight energy shift towards  $E_F$ . We assign this component to an fcc phase with random occupancy of octahedral and tetrahedral sites.

### 1. Introduction

Alkali-metal-intercalated  $\text{C}_{60}$  ( $\text{A}_x\text{C}_{60}$ ) has been subject to intensive study during the last few years, in part due to the high-temperature superconducting properties of  $\text{A}_3\text{C}_{60}$  [1, 2]. The electronic structure close to  $E_F$  can give important information to understand the superconducting properties of these quasimolecular compounds [3, 4]. The observed differences between the experimentally obtained width of the partially filled LUMO-derived band and that predicted on the basis of several theoretical approaches have not yet been thoroughly explained [4–6].

In order to correctly interpret photoemission spectra from  $\text{A}_3\text{C}_{60}$ , one has to ensure that the samples have been carefully prepared, since a lack of homogeneity can lead to a mixture of different phases with different compositions. The determination of an equilibrium phase diagram for the alkali– $\text{C}_{60}$  system is thus an important step towards correctly interpreting results obtained on  $\text{A}_3\text{C}_{60}$ . In a recent work, Poirier *et al* propose equilibrium phase diagrams for  $\text{A}_x\text{C}_{60}$  with  $\text{A} = \text{K}, \text{Rb},$  and  $\text{Cs}$ , and  $0 \leq x \leq 6$ , over a wide temperature range [7]. Since a lot of the data necessary to obtain such diagrams are still lacking, the authors had to speculate in order to cover the whole range of temperatures and compositions. But even for regions for which data are available there is still some controversy about the phase stabilities, especially in the region of low  $x$ . According to Poirier *et al*, in the case of Rb and Cs the  $\text{AC}_{60}$  phase is stable at room temperature, coexisting with  $\alpha\text{C}_{60}$  (a solid solution of the alkali metal in the  $\text{C}_{60}$  matrix) for  $x < 1$ , and with  $\text{A}_3\text{C}_{60}$  for  $x > 1$ . In the case of K, however, they suggest that  $\text{KC}_{60}$  is not stable at room temperature, but only above 425 K, where they find a rock-salt fcc phase with only

octahedral sites occupied. This high-temperature phase decomposes into  $\alpha\text{C}_{60}$  and  $\text{K}_3\text{C}_{60}$  below this temperature. This result contrasts with those of other studies, which propose that a  $\text{KC}_{60}$  phase does exist at room temperature and even at lower temperatures, though some controversy remains about the structure of this compound. According to Zhu *et al* [8], there exists a rhombohedral  $\text{KC}_{60}$  phase with  $2^\circ$  distortion from cubic symmetry at room temperature, which evolves into an fcc phase with random occupancy of tetrahedral and octahedral sites at intermediate temperatures (between 323 K and 393 K), and finally to the high-temperature fcc phase, with only octahedral sites occupied. Kälber *et al* report an orthorhombic  $\text{KC}_{60}$  phase with  $\text{sp}^3$  intermolecular bonds obtained by quenching from 420 K to room temperature, whereas by means of slow cooling they obtained  $\alpha\text{-C}_{60} + \text{K}_3\text{C}_{60}$  [9]. On the other hand, Petit *et al* found a dimeric phase below 280 K that changes at this temperature into an fcc phase, which is the equilibrium phase at room temperature. This fcc phase evolves into a polymeric phase with orthorhombic symmetry at 320 K, and finally into a high-temperature fcc phase at 360 K [10]. Zhu *et al* had previously reported that the polymeric phases are metastable at room temperature, while the dimeric phase appears below 270 K [11]. Pekker *et al* [12] report an equilibrium single-crystalline polymeric  $\text{KC}_{60}$  phase at room temperature, although an fcc phase can be obtained by quenching from 300 K.

From all of these studies, the existence of a room temperature  $\text{KC}_{60}$  phase is evident, though some questions concerning its symmetry and stability require further study. In this work, a photoemission study of the valence band of  $\text{K}_x\text{C}_{60}$  ( $0 \leq x \leq 3$ ) at room temperature is presented, with special emphasis on the LUMO-derived band close to the Fermi energy ( $E_F$ ). The evolution of this band with K doping confirms the existence of  $\text{KC}_{60}$  at room temperature. Two different components are observed in the LUMO-derived band, separated by 1 eV in binding energy, and assigned to two different  $\text{KC}_{60}$  phases with different symmetry and conducting character. The observation of the double peak is shown to be strongly dependent on the photon energy used.

## 2. Experimental details

$\text{K}_x\text{C}_{60}$  samples were prepared by *in situ* K evaporation from a SAES getter source onto a polycrystalline  $\text{C}_{60}$  film previously deposited on a Ta substrate, followed by ten minutes of annealing at 100 °C. The pressure rose from  $2 \times 10^{-10}$  mbar to  $1 \times 10^{-9}$  mbar during the K evaporation. To determine the K-doping level,  $x$ , we first measured *in situ* the resistivity of several samples prepared with different K concentrations until the maximum value,  $x = 6$ , was reached. At this point we took a photoemission spectrum and used the intensity of the LUMO-derived band as a reference. The minimum resistivity corresponded to a LUMO intensity that was approximately one half of the LUMO intensity of the  $\text{K}_6\text{C}_{60}$  sample and, consequently, to  $\text{K}_3\text{C}_{60}$ . We estimate the uncertainty in the determination of  $x$  to be  $\pm 0.2$  on the basis of the differences observed between the doping level of the minimum resistivity and that corresponding to one half of the LUMO intensity of  $\text{K}_6\text{C}_{60}$ . In order to avoid effects due to changes in the photoionization cross section, the same photon energy was used throughout the whole procedure of doping-level determination. Photoemission (PE) measurements were performed at the TGM5 monochromator of the Berliner Elektronenspeicherring für Synchrotronstrahlung (BESSY), using undulator radiation. An UHV chamber equipped with an angle-integrating hemispherical electron-energy analyser (VG-CLAM) was used. The PE spectra were taken in normal emission. The overall energy resolution was  $\sim 0.25$  eV.

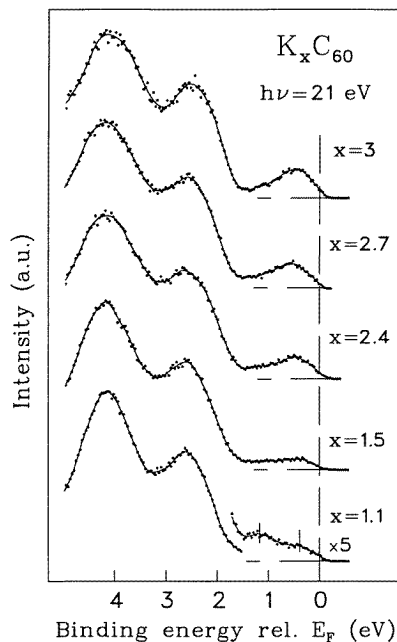


**Figure 1.** PE spectra of the region close to  $E_F$  for  $K_xC_{60}$  for different values of  $x$  between 1.1 and 3, taken at a photon energy of  $h\nu = 21$  eV.

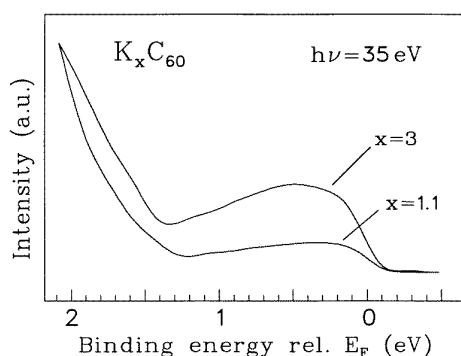


**Figure 2.** PE spectra at the LUMO-derived band region of  $K_xC_{60}$  for  $x = 1.1$  and  $x = 3$ , taken at a photon energy of  $h\nu = 35$  eV.

### 3. Results and discussion

In figure 1, photoemission spectra of  $K_xC_{60}$  for  $1 < x \leq 3$ , obtained with a photon energy of  $h\nu = 21$  eV, are shown. For  $K_3C_{60}$  the spectrum is very similar to other spectra reported in previous work, with an asymmetric and broad LUMO-derived band extending between  $E_F$  and 1.5 eV [13, 14]. For lower  $x$ -values the intensity of the LUMO gradually decreases, maintaining the same shape of the  $K_3C_{60}$  spectrum up to  $x \approx 2$ . Below this K concentration the LUMO asymmetric peak transforms into a flat structure (the spectrum for  $x = 1.5$ ), and finally into a double peak at  $x$ -values close to  $x = 1$  (the spectrum at the bottom of figure 1). A similar double structure has been reported by other authors for  $A_xC_{60}$  compounds with  $A = K, Rb,$  and  $Cs$ , and  $x$  close to 1 [15–17]. On the other hand, other photoemission studies of the same systems do not report any double peak for any doping level between 0 and 3 [18, 19]. Note that in these studies different photon energies were used. The photon energy employed in the PE experiments on  $C_{60}$  and its compounds is expected to play a very important role, since final-state effects caused by symmetry and parity selection rules of the molecular orbitals can lead to significant changes in the photoionization cross section [20]. In figure 2 we show a PE spectrum of two of the samples shown in figure 1, with  $x = 1.1$  and 3, taken at a photon energy of  $h\nu = 35$  eV. In both cases the spectral shape of the LUMO-derived band is different to that obtained with  $h\nu = 21$  eV. For  $x = 3$  the states at  $E_F$  have a higher intensity than in figure 1, allowing one to resolve the Fermi cut-off. For  $x = 1.1$  no double structure is resolved. These differences in the spectral lineshape with varying photon energy can explain why the double feature of the LUMO-derived band has only been reported in some studies.

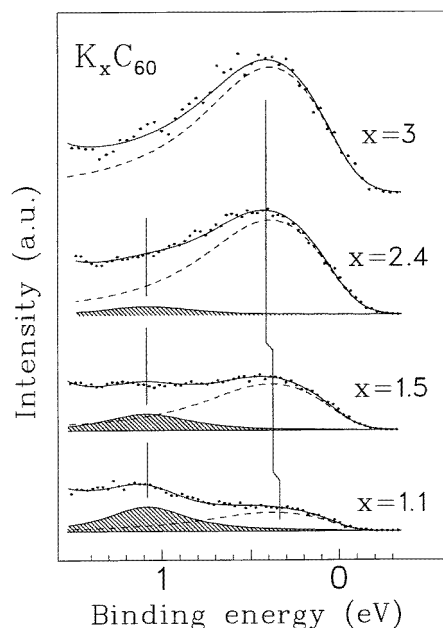


**Figure 3.** The results from a least-squares fitting procedure applied to the PE data of figure 1 in the region of the LUMO-derived band.

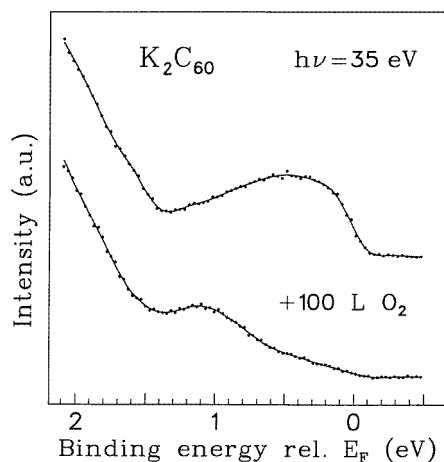


**Figure 4.** PE spectra of the LUMO-derived band region of a  $K_2C_{60}$  sample before and after exposure to 100 L  $O_2$ , taken at a photon energy of  $h\nu = 35$  eV.

In order to perform a more detailed analysis of the data shown in figure 1, a least-squares fitting procedure was carried out for the region of the LUMO-derived band. The fitting function consisted of two Lorentz lines multiplied by the Fermi function and convoluted with a Gaussian line to account for the experimental resolution. The contribution of the low-energy tail of the HOMO peak was also taken into account by introducing a Lorentz line in the fitting function with fixed parameters taken from the corresponding wide-energy-range spectra. A Shirley background function was used to approximate the effect of inelastic electrons [21]. Figure 3 shows the results of such a fitting analysis. For the lowest doping level studied,  $x = 1.1$ , the two peaks observed in figure 1 are clearly resolved. Their binding energy positions are 1.08 eV (shaded component) and 0.33 eV (dashed component), and the intensity of the shaded subspectrum is higher than that of the dashed one. In the spectrum for  $x = 1.5$ , the low-binding-energy line predominates, and the intensity of the high-binding-energy component decreases with respect to the  $x = 1.1$  case. The same trend continues for  $x = 2.4$ , and, finally, for  $x = 3$ , the shaded component is completely absent. These results indicate that at low doping levels two phases coexist: a conducting phase, which evolves towards  $K_3C_{60}$  at higher  $x$ -values; and a phase with no states at  $E_F$ , which gradually disappears when  $x$  increases.

A significant result of the fitting analysis is that the binding energy position of the dashed component could not be kept constant for all of the spectra. In a first attempt, the energy position and width of the low-energy component were set to the corresponding values for the  $K_3C_{60}$  phase ( $E_B = 0.41$  eV). However, by fixing the energy position of this component in the spectrum for  $x = 1.1$  to this value, a  $\sim 20\%$  increase of  $\chi^2$  was observed as compared to the value obtained by leaving this parameter free. The value obtained in this case,  $E_B = 0.33$  eV, is shifted  $\sim 0.1$  eV with respect to that for the  $x = 3$  case. The energy

position of this component for  $x = 2.4$  is the same as for  $x = 3$ , whereas for  $x = 1.5$  it has an intermediate value between that for  $x = 1.1$  and that for  $x = 3$  ( $E_B = 0.38$  eV). Assuming that the spectrum for  $x = 3$  corresponds to pure  $K_3C_{60}$ , the observed binding energy shift would indicate that, at low K concentrations, the low-binding-energy component cannot be assigned to  $K_3C_{60}$ . On the other hand, the only difference with respect to  $K_3C_{60}$  is this small binding energy shift, i.e. the electronic properties of this phase should be very similar to those of  $K_3C_{60}$ .

According to some previous work, for  $x$ -values close to 1, two different phases may be obtained. Petit *et al* [10] reported an fcc random phase at room temperature, a dimeric phase for lower temperatures, and an orthorhombic, polymeric  $KC_{60}$  phase for  $T > 50$  °C. On the other hand, Pekker *et al* [12] reported an equilibrium polymeric  $KC_{60}$  phase at room temperature, but an fcc random phase may also be obtained at room temperature by quenching from higher temperatures. These different results suggest that both an fcc phase with random occupancy of tetrahedral and octahedral sites, and an orthorhombic (polymeric or dimeric)  $KC_{60}$  phase may be obtained at room temperature. The relative amounts of the two phases seem to be strongly dependent on the preparation conditions. Under the present ones, the two phases seem to coexist for  $x$ -values lower than 2, as is indicated by the presence of the two different photoemission components in figure 3. The low-binding-energy component approaches  $K_3C_{60}$  with increasing K doping, and, consequently, it can be assigned to the fcc random phase, where the K atoms should have symmetry and electronic properties similar to those of  $K_3C_{60}$ . The observed binding energy shift of this phase with respect to  $K_3C_{60}$  might be associated with the partial occupancy of the K sites, since it disappears gradually, as is illustrated by the intermediate value obtained for  $x = 1.5$ .

The high-binding-energy component should be assigned to the orthorhombic  $KC_{60}$  phase. The presence of a dimeric phase at room temperature should be excluded, since this phase appears only at temperatures below 280 K [10, 11]. The higher-binding-energy position of this phase with respect to the fcc phase must be explained in terms of a different bonding mechanism. Whereas the fcc phase constitutes a three-dimensional network, the orthorhombic  $KC_{60}$  phase can be regarded as formed from separate, one-dimensional chains of  $KC_{60}$  units. The HOMO–LUMO gap of a  $C_{60}^-$  isolated ion is 1.9 eV [22], significantly lower than the HOMO–LUMO gap of  $K_3C_{60}$  (2.5 eV, as shown in figure 1), and much closer to the HOMO–LUMO gap of the orthorhombic  $KC_{60}$  phase (1.6 eV). This suggests that the electronic configuration of this phase resembles more the situation of the isolated  $C_{60}^-$  ion than that of the three-dimensional  $K_3C_{60}$  phase.

A further argument supporting the assignment of the two components observed in figure 3 to an fcc phase and an orthorhombic  $KC_{60}$  phase, respectively, is found by exposing  $K_xC_{60}$  to oxygen. Figure 4 shows PE spectra of a  $K_2C_{60}$  sample taken at  $h\nu = 35$  eV before and after exposure to 100 L  $O_2$ . Note that, at this photon energy, the double structure cannot be resolved (see figure 2). After oxygen exposure, however, the  $KC_{60}$  component becomes visible, whereas the fcc phase disappears. According to Pekker *et al* [12], the orthorhombic  $KC_{60}$  phase is stable in air for hours, i.e. it is highly resistant to oxidation. On the other hand, the fcc phase should behave like  $K_3C_{60}$ , which has a very high tendency to oxidize.

#### 4. Conclusions

We have investigated the electronic structure of  $K_xC_{60}$  at room temperature. At low doping levels ( $x \sim 1$ ), we have found two coexisting phases with different LUMO-derived band positions. The PE cross section of the corresponding peaks is strongly dependent on the photon energy employed, allowing one to resolve them only for certain photon energies. We

have assigned the component with the lower-binding-energy LUMO to an fcc phase with random occupancy of tetrahedral and octahedral sites, and that with the higher-binding-energy LUMO to an orthorhombic (dimeric or polymeric)  $\text{KC}_{60}$  phase. With increasing doping, the fcc phase evolves towards  $\text{K}_3\text{C}_{60}$ , while the  $\text{KC}_{60}$  phase gradually disappears. The  $\text{KC}_{60}$  phase is highly resistant to oxidation as shown by the photoemission spectrum taken after exposure to 100 L  $\text{O}_2$ .

### Acknowledgments

The authors wish to thank the BESSY staff for technical assistance. Fruitful discussions with G Kaindl are also gratefully acknowledged.

### References

- [1] Hebard A F, Rosseinsky M J, Haddon R C, Murphy D W, Glarum S H, Palstra T T M, Ramirez A P and Kortan A R 1991 *Nature* **350** 600
- [2] Rosseinsky M J *et al* 1991 *Phys. Rev. Lett.* **66** 2830
- [3] Takahashi T *et al* 1991 *Physica C* **185–189** 417
- [4] Knupfer M, Merkel M, Golden M S, Fink J, Gunnarsson O and Antropov V P 1993 *Phys. Rev. B* **47** 13 944
- [5] Benning P J, Stepniak F, Poirier D M, Martins J L, Weaver J H, Chibante L P F and Smalley R E 1993 *Phys. Rev. B* **47** 13 843
- [6] Molodtsov S L *et al* 1993 *Z. Phys. B* **92** 347
- [7] Poirier D M, Owens D W and Weaver J H 1995 *Phys. Rev. B* **51** 1830
- [8] Zhu Q, Zhou O, Fischer J E, McGhie A R, Romanow W J, Strongin R M, Cichy M A and Smith A B III 1993 *Phys. Rev. B* **47** 13 948
- [9] Kälber T, Zimmer G and Mehring M 1995 *Phys. Rev. B* **51** 16 471
- [10] Petit P, Robert J and Fischer J E 1995 *Phys. Rev. B* **51** 11 924
- [11] Zhu Q, Cox D E and Fischer J E 1995 *Phys. Rev. B* **51** 3966
- [12] Pekker S, Jánossy A, Mihaly L, Chauvet O, Carrard M and Forró L 1994 *Science* **265** 1077
- [13] Seta M D and Evangelisti F 1995 *Phys. Rev. B* **51** 1096
- [14] Merkel M, Knupfer M, Golden M S, Fink J, Seemann R and Johnson R L 1993 *Phys. Rev. B* **47** 11 470
- [15] Takahashi T *et al* 1991 *Physica C* **185–189** 417
- [16] Seta M D and Evangelisti F 1993 *Phys. Rev. Lett.* **71** 2477
- [17] Seta M D and Evangelisti F 1995 *Phys. Rev. B* **51** 6852
- [18] Benning P J *et al* 1992 *Phys. Rev. B* **45** 6899
- [19] Gu C *et al* 1992 *Phys. Rev. B* **45** 6348
- [20] Benning P J, Poirier D M, Martins J L, Weaver J H, Hauffer R E, Chibante L P F and Smalley R E 1991 *Phys. Rev. B* **44** 1962
- [21] Shirley D A 1972 *Phys. Rev. B* **5** 4709
- [22] Yang S H, Pettiette C L, Conceicao J, Cheshnovsky O and Smalley R E 1987 *Chem. Phys. Lett.* **139** 233